DEUTSCHES ELEKTRONEN-SYNCHROTRON **DESY**

DESY 87-039
May 1987

TWO PION PRODUCTION IN PHOTON PHOTON COLLISIONS

by

J. Bijnens, F. Cornet

Deutsches Elektronen-Synchrotron DESY, Hamburg

ISSN 0418-9833

NOTKESTRASSE 85 · 2 HAMBURG 52

To be sure that your preprints are promptly included in the
HIGH ENERGY PHYSICS INDEX ,
send them to the following address (if possible by air mail) :

DESY
Bibliothek
Notkestrasse 85
2 Hamburg 52
Germany

DESY 87-039
May 1987

ISSN 0418-9833

Two pion production in photon photon collisions

Johan Bijnens and Fernando Cornet*

Deutsches Elektronen-Synchrotron DESY, Hamburg, FRG

Abstract

We calculate within chiral perturbation theory the cross-section for $\gamma\gamma \to \pi^0\pi^0$ and $\gamma\gamma \to \pi^+\pi^-$ to next to leading order. The first process only depends on the one loop contributions and forms a test of chiral perturbation theory. We also calculate the pion electromagnetic formfactor and compare it to recent data.

* On leave from Departamento de Fisica Teórica, Universidad Autónoma de Barcelona (Spain)

1. Introduction

The processes $\gamma\gamma \to \pi^+\pi^-$ and $\gamma\gamma \to \pi^0\pi^0$ have been measured at e^+e^- colliders for center of mass energies $W_{\gamma\gamma} \lesssim 3$ GeV. The latter process has been observed by the Crystal Ball collaboration [1] with a significant $\pi^0\pi^0$ continuum below the $f_2(1270)$ peak. The experimental situation for low mass $\pi^+\pi^-$ pairs is somewhat confused. The data [2, 3] seem to show a large enhancement above threshold. A dip [2] just below the f_2 resonance was not confirmed by TPC/$\gamma\gamma$ and DELCO [4].

On the theoretical side there exist calculations for high mass $\pi^+\pi^-$ and $\pi^0\pi^0$ pairs [5] within perturbative QCD. The Born approximation, assuming point like pions and no final state interactions was calculated long ago [6]. It cannot explain the enhancement near threshold. One can include final state interactions if one assumes that the production cross-section is given by the pointlike cross-section. The final state interactions can then be expressed in terms of the $\pi\pi$ phase shifts. The latest analysis was done in [7]. Using similar assumptions an enhancement of $\pi^+\pi^-$ production near threshold was obtained with an attractive $\pi\pi$ potential [8]. In this reference the $\pi^0\pi^0$ cross-section remained small.

In this paper we include both the final state interactions and the deviation from the QED vertex using chiral perturbation theory [9,10]. Our results show a moderate enhancement for $\pi^+\pi^-$ production near threshold and a small steadily rising cross-section for $\pi^0\pi^0$ production. The one loop result for $\pi^0\pi^0$ production only depends on the pion decay constant and meson masses. It is independent of all new parameters appearing at this order of chiral perturbation theory and thus provides a clean experimental test of this formalism. The production of $\pi^+\pi^-$ pairs depends on two extra constants. These can be fixed via other experiments. The structure dependent term in $\pi \to e\nu\gamma$ depends on exactly the same combination of the new parameters as $\gamma\gamma \to \pi^+\pi^-$.

In section 2 we give a short review of chiral perturbation theory and calculate as an example the pion electromagnetic form factor. We also fit this to recent data [13] to determine one of the constants. In section 3 we give a short proof that $\pi^0\pi^0$ production does not depend on any additional parameters at this order of chiral perturbation theory and calculate the amplitude. In section 4 we calculate the cross-section for $\pi^+\pi^-$ production and compare it with experimental data and we present our conclusion in the final section.

2. Chiral perturbation theory

The QCD Lagrangian is for vanishing quark masses symmetric under chiral $SU(3)_L \times SU(3)_R$ transformations. This symmetry is spontaneously broken to $SU(3)_V$. The 8 Goldstone bosons associated with this breakdown are identified with the pseudoscalar mesons π, K, η. These can be conveniently parametrized using a 3 x 3 matrix

$$\Sigma = \exp(2iM/f)$$

$$M = \begin{pmatrix} \frac{\pi^0}{\sqrt{2}} + \frac{\eta}{\sqrt{6}} & \pi^+ & K^+ \\ \pi^- & -\frac{\pi^0}{\sqrt{2}} + \frac{\eta}{\sqrt{6}} & K^0 \\ K^- & \bar{K}^0 & -\sqrt{\frac{2}{3}}\,\eta \end{pmatrix}.$$

Σ transforms linearly under $SU(3)_L \times SU(3)_R$ via

$$\Sigma \to L \Sigma R^\dagger.$$

Chiral symmetry is also explicitly broken by quark masses and the electromagnetic interaction. The most general Lagrangian consistent with chiral and Lorentz invariance, U(1) gauge invariance and P, C and T to lowest order in e^2, quark masses and momenta is

$$\mathcal{L}_2 = \frac{f^2}{8} \mathrm{tr}\left(D_\mu \Sigma D^\mu \Sigma^\dagger\right) + v_1 \mathrm{tr}\left[m(\Sigma + \Sigma^\dagger)\right] + v_2 e^2 \mathrm{tr}\left(Q\Sigma Q\Sigma^\dagger\right) - \frac{1}{4} F^2. \quad (1)$$

We used the notation

$$D_\mu \Sigma = \partial_\mu \Sigma + ie\left[Q, \Sigma\right] A_\mu$$

$$m = \begin{pmatrix} m_u & & \\ & m_d & \\ & & m_s \end{pmatrix} \qquad Q = \begin{pmatrix} 2/3 & & \\ & -1/3 & \\ & & -1/3 \end{pmatrix} \quad (2)$$

and F^2 is the photon field strength squared.

The first term in (1) provides the kinetic energy term for the mesons and the interaction terms consistent with current algebra. The second term transforms as $(3_L, \bar{3}_R) + (\bar{3}_L, 3_R)$ under $SU(3)_L \times SU(3)_R$ and describes the explicit breaking of chiral symmetry by the quark masses. The third term transforms as $(8_L, 8_R)$ and describes the leading electromagnetic effects in purely hadronic quantities. At this level f, v_1 and v_2 can be fixed using the pion decay constant and the meson masses

$$f = f_\pi \;;\; v_1 = \frac{m_{K^0}^2}{4(m_d + m_s)} = \frac{m_{\pi^0}^2}{4(m_u + m_d)} = \frac{3 m_\eta^2}{4(m_u + m_d + 4 m_s)}$$

$$v_2 = \frac{f^2}{2}\left(m_{\pi^+}^2 - m_{\pi^0}^2\right) = \frac{f^2}{2}\left(m_{K^+}^2 - m_{K^0}^2\right). \quad (3)$$

In this paper we keep $m_u = m_d$ so isospin is only broken by the electromagnetic interaction. The term proportional to v_2 is a correction of $O(e^2)$ and does not contribute to $\gamma\gamma \to \pi\pi$ at $O(e^2)$. Tree level diagrams in $\mathcal{L}_2$ give the current algebra predictions up to $O(p^2, m_i^2)$ with p^2 a typical external momentum. Loop diagrams with vertices from $\mathcal{L}_2$ give contributions of $O(p^4, p^2 m_i^2, m_i^4)$.

There are also contributions of this order from higher order terms in the Lagrangian. All possible terms up to this order have been given in [9]:

$$\begin{aligned} \mathcal{L}_4 = {} & L_1\left[\mathrm{tr}\left(D_\mu \Sigma D^\mu \Sigma^\dagger\right)\right]^2 + L_2\left[\mathrm{tr}\left(D_\mu \Sigma D_\nu \Sigma^\dagger\right)\right]^2 + \\ & + L_3\left[\mathrm{tr}\left(D_\mu \Sigma D^\mu \Sigma^\dagger\right)^2\right] + L_4 \mathrm{tr}\left[D_\mu \Sigma D^\mu \Sigma^\dagger\right] \mathrm{tr}\left[m\Sigma + m\Sigma^\dagger\right] + \\ & + L_5 \mathrm{tr}\left[D_\mu \Sigma D^\mu \Sigma^\dagger (m\Sigma^\dagger + \Sigma m)\right] + L_6\left[\mathrm{tr}\left(m\Sigma + m\Sigma^\dagger\right)\right]^2 + \\ & + L_7\left[\mathrm{tr}\left(m\Sigma - m\Sigma^\dagger\right)\right]^2 + L_8 \mathrm{tr}\left[m\Sigma m\Sigma + m\Sigma^\dagger m\Sigma^\dagger\right] + \\ & + i L_9\left[\mathrm{tr}\left(F_{\mu\nu}^L D^\mu \Sigma D^\nu \Sigma^\dagger\right) + \mathrm{tr}\left(F_{\mu\nu}^R D^\mu \Sigma^\dagger D^\nu \Sigma\right)\right] + \\ & + L_{10} \mathrm{tr}\left[F_{\mu\nu}^L \Sigma F^{\mu\nu R} \Sigma^\dagger\right] + L_{11} \mathrm{tr}\left[F_{\mu\nu} F^{\mu\nu}\right] + L_{12} \mathrm{tr}\left[m^2\right]. \end{aligned} \quad (4)$$

The L_i are arbitrary constants, which will allow us to absorb all divergences appearing in one loop diagrams with $\mathcal{L}_2$ vertices [10]. Using dimensional regularization the bare coupling constants L_i are redefined

$$L_i = L_i^r - \Gamma_i \frac{1}{32\pi^2}\left(\frac{1}{\varepsilon} + \ln 4\pi - \ln\mu^2 + 1 - \gamma\right), \tag{5}$$

where L_i^r are the coupling constants renormalized at scale μ and

$$\begin{aligned} &\Gamma_1 = 3/32 \quad \Gamma_2 = 3/16 \quad \Gamma_3 = 0 \quad \Gamma_4 = 1/8 \\ &\Gamma_5 = 3/8 \quad \Gamma_6 = 11/144 \quad \Gamma_7 = 0 \quad \Gamma_8 = 5/48 \\ &\Gamma_9 = 1/4 \quad \Gamma_{10} = -1/4 \quad \Gamma_{11} = -1/8 \quad \Gamma_{12} = 5/24 . \end{aligned} \tag{6}$$

The coefficients L_{11} and L_{12} are purely external field subtractions and do not contribute to physical quantities [9]. The values of the renormalized coupling constants L_i^r have to be fixed from experimental data.

In addition there are terms describing the effects of the anomaly [11]. These can be written in the form [11]

$$\mathcal{L}_{WZ} = \varepsilon^{\mu\nu\alpha\beta} B_{\mu\nu\alpha\beta} \tag{7}$$

where $B_{\mu\nu\alpha\beta}$ depends on the meson fields, momenta and external fields and does not contain any Levi Civita tensors.

As an example let us calculate the pion electromagnetic structure function [12], defined by $\langle\pi^+(p')|J^\mu_{em}|\pi^+(p)\rangle = -F_\pi(q^2)\,(p+p')^\mu$, with $q^2 = (p+p')^2$. To lowest order it is just the photon vertex so $F(q^2)=1$. At order m^2, p^2 there are corrections from wave function renormalization and the 1 particle irreducible graphs in fig.1. In calculating this we observe that all infinities cancel and obtain

$$F_\pi(q^2) = 1 + \frac{4}{f^2} L_9^r\, q^2 + \frac{1}{16\pi^2 f^2}\left(2m_\pi^2 H\left(\frac{q^2}{m_\pi^2}\right) + m_K^2 H\left(\frac{q^2}{m_K^2}\right) - \frac{1}{3}q^2 \ln\frac{m_\pi^2}{\mu^2} - \frac{1}{6}q^2 \ln\frac{m_K^2}{\mu^2}\right) \tag{8}$$

with

$$H(x) = -\frac{4}{3} + \frac{5}{18}x + \left(\frac{2}{3} - \frac{1}{6}x\right)\sqrt{\frac{x-4}{x}}\,\ln Q(x)$$

$$Q(x) = \frac{\sqrt{x-4} + \sqrt{x}}{\sqrt{x-4} - \sqrt{x}} . \tag{9}$$

For small q^2 this is related to the charge radius of the pion*

$$F_\pi(q^2) = 1 + \frac{1}{6}\langle r_\pi^2\rangle q^2 =$$

$$= 1 + q^2\left[\frac{4}{f^2}L_9^r + \frac{1}{16\pi^2 f^2}\left(-\frac{1}{3}\ln\frac{m_\pi^2}{\mu^2} - \frac{1}{6}\ln\frac{m_K^2}{\mu^2} - \frac{1}{2}\right)\right]. \tag{10}$$

Using the measured value of the pion electromagnetic radius [13]

$$r^2 = 0.439 \pm 0.008\ \text{fm}^2$$

we get

$$L_9^r = (7.7 \pm 0.2).10^{-3} \tag{11}$$

for a renormalization scale $\mu^2 = m_\eta^2$.

The values used are $f_\pi = 134$ MeV, $m_\pi = 137$ MeV, $m_K = 494$ MeV and $m_\eta = 549$ MeV. We have also performed a fit of the complete formula (10) to the data of ref. 13 . The results of the fit are displayed in fig.2. The result of the fit with $|F_\pi(0)|^2 = 1$ leads to

$$L_9^r = (6.8 \pm 0.2) \times 10^{-3} . \tag{12}$$

The dashed line in fig.2 is the fit of eq.(8) but with the overall normalization free. The preferred normalization $n = 0.980 \pm 0.003$ of the fit is however outside the normalization quoted in [13]. This fit gave a value 6.3×10^{-3} for L_9^r.

In section 4 we will need the value of the constant $L_9^r + L_{10}^r$. From [9,12] we find that the structure dependent term in $\pi \to e\nu\gamma$ depends on the same combination. From the data (see [9]) we obtain

$$L_9^r + L_{10}^r = (1.4 \pm 0.4) \times 10^{-3} . \tag{13}$$

3. $\gamma\gamma \to \pi^0\pi^0$

We first prove that there are no $\pi^0\pi^0\gamma$ or $\pi^0\pi^0\gamma\gamma$ vertices in $\mathcal{L}_2$ or $\mathcal{L}_4$**, so no tree level diagram contributes to this process. Couplings to photons come from insertions of $F_{\mu\nu}$ and/or $D_\mu \Sigma$. Since Σ is diagonal, when only π^0 fields contribute, and Q is a diagonal matrix (eq.2),

$$D_\mu (\pi^0) = \partial_\mu \Sigma(\pi^0) + ie A_\mu [Q, \Sigma(\pi^0)] = \partial_\mu \Sigma(\pi^0).$$

So terms containing only covariant derivatives cannot generate couplings $\pi^0\pi^0\gamma$ nor $\pi^0\pi^0\gamma\gamma$. The term corresponding to L_9 vanishes for a diagonal $\Sigma(\pi^0)$ because $F_{\mu\nu}$ is contracted to a symmetric tensor in that case. The L_{10} term can be rewritten as

$$L_{10} F_{\mu\nu} F^{\mu\nu} \mathrm{tr}[Q\Sigma Q\Sigma^+] = \frac{1}{2} L_{10} F_{\mu\nu} F^{\mu\nu} \left\{ \mathrm{tr}([Q,\Sigma][Q,\Sigma^+]) - 2\,\mathrm{tr}\,Q^2 \right\} \quad (14)$$

which clearly vanishes for $\Sigma(\pi^0)$.

The contributions from $\mathcal{L}_{WZ}$ always involve $\varepsilon_{\mu\nu\alpha\beta}$ so a contribution from the anomaly to the process $\gamma\gamma \to \pi\pi$ is forbidden by parity. The only contribution to $\sigma(\gamma\gamma \to \pi^0\pi^0)$ comes from the loop-diagrams drawn in fig.3, where the particles propagating in the loops are charged pions or kaons. Note that, since there are no counterterms available to cancel the divergences in this channel, we expect the result of the one loop calculation to be finite.

We choose a reference frame where the photon polarization vectors $\varepsilon_{1,2}$ satisfy

$$k_1 \cdot \varepsilon_1 = k_1 \cdot \varepsilon_2 = k_2 \cdot \varepsilon_1 = k_2 \cdot \varepsilon_2 = 0 \quad (15)$$

where k_1, k_2 are the momenta of the incoming photons. In this frame the amplitude due to pion loops is

$$A_\pi = 4\, i\, e^2\, \varepsilon_1 \cdot \varepsilon_2 \frac{1}{16\pi^2 f^2} (1 - s_\pi) \left(1 + \frac{1}{s_\pi} \ln^2 Q_\pi\right) \quad (16)$$

and the amplitude due to kaon loops is

$$A_K = -i e^2\, \varepsilon_1 \cdot \varepsilon_2 \frac{1}{16\pi^2 f^2} s \left[1 + \frac{1}{s_K} \ln^2 Q_K\right] \quad (17)$$

Using $s = (k_1 + k_2)^2$, the center of mass energy squared. The symbols used in eqs.16,17 are

$$s_i = \frac{s}{m_i}$$

$$Q_i = \frac{\sqrt{s_i - 4} + \sqrt{s_i}}{\sqrt{s_i - 4} - \sqrt{s_i}} \quad (18)$$

for $i = \pi, K$.

This disagrees with the expression obtained in [14]. The authors of ref. 14 did not include the diagrams in fig.3a,b and used a different breaking of chiral symmetry by meson masses.

From this amplitude one can calculate the total cross-section $\sigma(\gamma\gamma \to \pi^0\pi^0)$ shown in fig.4 (solid line). The pion loops contribution (dashed line) dominates the cross-section, while the kaon loops are numerically rather small although their interference with the π-loops causes an appreciable decrease in σ. The amplitude in eqs.16,17 is purely S-wave, so there is no dependence on the scattering angle in the $\gamma\gamma$ center of mass system. Unfortunately, we cannot compare our results with Crystal Ball data because they are not yet absolutely normalized.

This result is based on an expansion in quark masses and external momenta. To establish its region of validity would require a calculation of the next order. This is beyond the scope of this paper. Experience with chiral symmetry leads us to expect that this result will be reliable up to center of mass energies of 500-700 MeV. The lower bound follows from the general agreement with chiral symmetry arguments in kaon decays. Another criterium is that the low energy expansion fails as soon as resonance behaviour becomes important. The first resonance in this process appears around 1 GeV so the above bound should be reliable.

4. $\gamma\gamma \to \pi^+\pi^-$

This process does already occur at tree level in the chiral Lagrangian. The amplitude at tree level is given by [6]

$$A_{\gamma\gamma\to\pi^+\pi^-} = 2ie^2 \left\{ \varepsilon_1\cdot\varepsilon_2 - \frac{p_+\cdot\varepsilon_1\; p_-\cdot\varepsilon_2}{p_+\cdot k_1} - \frac{p_+\cdot\varepsilon_2\; p_-\cdot\varepsilon_1}{p_+\cdot k_2} \right\}$$

$k_{1,2}$ are the momenta of the incoming photons, p_+, p_- are the momenta of the outgoing π^+, π^- and $\varepsilon_1, \varepsilon_2$ are the polarization vectors of the photons. In addition to the graphs of fig.3 this process also gets contributions from wave function renormalization and the graphs in fig.5. The loops now also involve π°, k° and η contributions and not only π^+, k^+ contributions as in the $\pi^\circ\pi^\circ$ case. Meson loop corrections to the photon wavefunction renormalization are a correction of $O(e^2)$ to the Born approximation so we don't include them. In addition there is also a dependence on $\mathcal{L}_4$ but not on $\mathcal{L}_{WZ}$. The latter has no contributions because of parity conservation (see section 3). The amplitude including the next order can be written as

$$A_{\gamma\gamma\to\pi^+\pi^-} = 2ie^2 \left\{ a\,\varepsilon_1\cdot\varepsilon_2 - \frac{p_+\cdot\varepsilon_1\; p_-\cdot\varepsilon_2}{p_+\cdot k_1} - \frac{p_+\cdot\varepsilon_2\; p_-\cdot\varepsilon_1}{p_+\cdot k_2} \right\} \qquad (19)$$

in the same frame as used in section 3 (eq.15).
Where a is given by

$$a = 1 + \frac{4s}{f^2}\left(L_9^r + L_{10}^r\right) - \frac{1}{16\pi^2 f^2}\left(\frac{3}{2}s + m_\pi^2 \ln^2 Q_\pi + \frac{1}{2} m_K^2 \ln^2 Q_K\right) \qquad (20)$$

using the same notation Q_i as in section 3. Squaring and averaging over photon helicities leads to a differential cross-section

$$\frac{d\sigma}{d\cos\theta} = \frac{\pi\alpha^2}{2s}\beta \left\{ 2|a|^2 - \mathrm{Re}\, a\, \frac{4\beta^2\sin^2\theta}{1-\beta^2\cos^2\theta} + \frac{4\beta^4\sin^4\theta}{(1-\beta^2\cos^2\theta)^2} \right\}. \qquad (21)$$

In (21) β is the velocity of the pions in the center of mass frame and θ the scattering angle.

The angular integration over θ can be performed and leads to

$$\sigma(s) = \frac{\pi\alpha^2}{2s}\beta \left\{ 4|a|^2 - 4(2-\delta)\,\mathrm{Re}\, a + 4\left(2 - 2\delta + (1-\beta^2)\left(1 + \frac{\delta}{2}\right)\right)\right\} \qquad (22)$$

with

$$\delta = \frac{1-\beta^2}{\beta} \ln\frac{1+\beta}{1-\beta}. \qquad (23)$$

This is plotted in fig.6 together with the Born cross-section (a=1) and values for $L_9^r + L_{10}^r = 1.4 \times 10^{-3}$. The position of the peak did not change from $W_{\gamma\gamma}$ = 306 MeV but its value increased by 13% from 476 to 539 nb. Notice from (5) and (6) that $L_9^r + L_{10}^r = L_9 + L_{10}$ so the value of this sum is renormalization scale independent. It is determined from the measurement of $\pi \to e\nu\gamma$ (see section 2). The size of the correction is rather insensitive to the precise value of this coefficient within errors.

In fig. 7 we compare our result with the available data. We have not compared our results to the DM1,2 results [3] because they do not show an absolutely normalized cross-section. In fig. 7a we have plotted the differential cross-section at a CMS scattering angle of 90°. The near threshold enhancement we obtained is not sufficient to explain the PLUTO data[2]. Fig.7b shows the cross-section integrated over $|\cos\theta_{CMS}| < 0.6$ and the TPC/$\gamma\gamma$ data [3]. They are obviously consistent with our result. In this region the loop corrections are very small.

5. Conclusion

We have calculated the next to leading order in chiral perturbation theory prediction for $\gamma\gamma \to \pi^0\pi^0$ and $\gamma\gamma \to \pi^+\pi^-$. A measurement of the former process at low center of mass energies (below 700 MeV) provides a stringent test for the loop expansion within chiral Lagrangians since it does not depend on any of the parameters present in $\mathcal{L}_4$. A typical cross-section of $\sim$ 10 nb was obtained at about 450 MeV slowly rising with $W_{\gamma\gamma}$.

A small enhancement for $\gamma\gamma \to \pi^+\pi^-$ was obtained near threshold, 13% at the peak of the cross-section for the central value of earlier determinations of the constants $L_9^r + L_{10}^r$. Changing this constant within errors did not enhance the cross-section enough to coincide with the data [3]. The rather large errors on the data do not allow to make any firm conclusion about failure of the theory. The corrections are small even up to rather large 700 MeV center of mass energies indicating that the expansion in quark masses and momenta is valid for this process.

Acknowledgements

We thank J. Gasser, H. Joos and H. Leutwyler for useful conversations. J.B. thanks D. Wyler and C. Schmidt at ETH Zürich where part of this job was done for hospitality. F.C. acknowledges financial support by Spanish Ministerio de Educación y Ciencia.

Footnotes

* For a discussion on how the ρ contributes in this approach see ref. 12, appendix C.

** A similar proof can be given for the $\pi^0\eta$, $\eta\eta$ and $K^0\bar{K}^0$ final states. These final states occur however only at high center of mass energy where the validity of the low energy expansion used here is not obvious.

References

1 Crystal Ball Collaboration, presented at Berkeley, june '86.

2 PLUTO Collaboration, C. Berger et al., Z. Phys. C26 (1984) 199.

3 DM1 Collaboration, A. Courau et al., Nucl. Phys. B271 (1986) 1;
DM2 Collaboration, Z. Ajaltouni et al., presented at Int. Symp. on Lepton Photon interactions, Kyoto (1985).

4 TPC/ Collaboration, H. Aihara et al., Phys. Rev. Lett. 57 (1986) 404;
DELCO Collaboration, R.P. Johnson et al., SLAC 294 (1986).

5 S. Brodsky, P. Lepage, Phys. Rev. D24 (1981) 1808.

6 S. Brodsky et al., Phys. Rev. D4 (1971) 1532.

7 C. Mennessier, Z. Phys. C16 (1983) 241.

8 T. Barnes et al., Phys. Lett. 183B (1987) 210.

9 J. Gasser, H. Leutwyler, Nucl. Phys. B250 (1985) 465.

10 S. Weinberg, Physica 96A (1979) 327.

11 J. Wess, B. Zumino, Phys. Lett. 37B (1971) 95;
E. Witten, Nucl. Phys. B223 (1983) 422.

12 J. Gasser, H. Leutwyler, Ann. of Physics 158 (1984) 142.

13 NA7 Collaboration, S.R. Amendolia et al., Nucl. Phys. B277 (1986) 168.

14 M.K. Volkov, V.N. Pervushin, Sov. J. Nucl. Phys. 22 (1976) 179.

Figure captions

Fig.1 One loop Feynman diagrams for the pion electromagnetic form factor.

Fig.2 A fit of the form factor to the data of ref.7. Plotted is the pion form factor squared, $|F_\pi|^2$. The full line is the fit with $|F_\pi^2(0)| = 1$ and the dashed line with the overall normalization of $|F_\pi^2|$ free.

Fig.3 One loop Feynman diagrams for $\gamma\gamma \to \pi^0\pi^0$.

Fig.4 The total cross-section $\gamma\gamma \to \pi^0\pi^0$ (Full line) for center of mass energies $W_{\gamma\gamma}$ from threshold to 0.7 GeV. The dashed line is the contribution of the π-loops.

Fig.5 One loop diagrams for $\gamma\gamma \to \pi^+\pi^-$ in addition to those of fig.4.

Fig.6 The total cross-section $\gamma\gamma \to \pi^+\pi^-$ for center of mass energies $W_{\gamma\gamma}$ from threshold to 0.7 GeV for $L_9^r + L_{10}^r = 1.4 \times 10^{-3}$. The dashed line is the Born cross-section.

Fig.7 a) Comparison with PLUTO data of the differential cross-section at $\cos\theta_{CM} = 0$.

b) Comparison with TPC/$\gamma\gamma$ data of the cross-section integrated over $|\cos\theta_{CM}| < 0.6$.

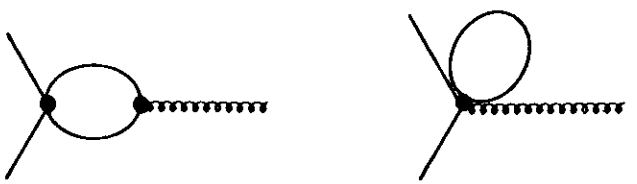

Fig. 1

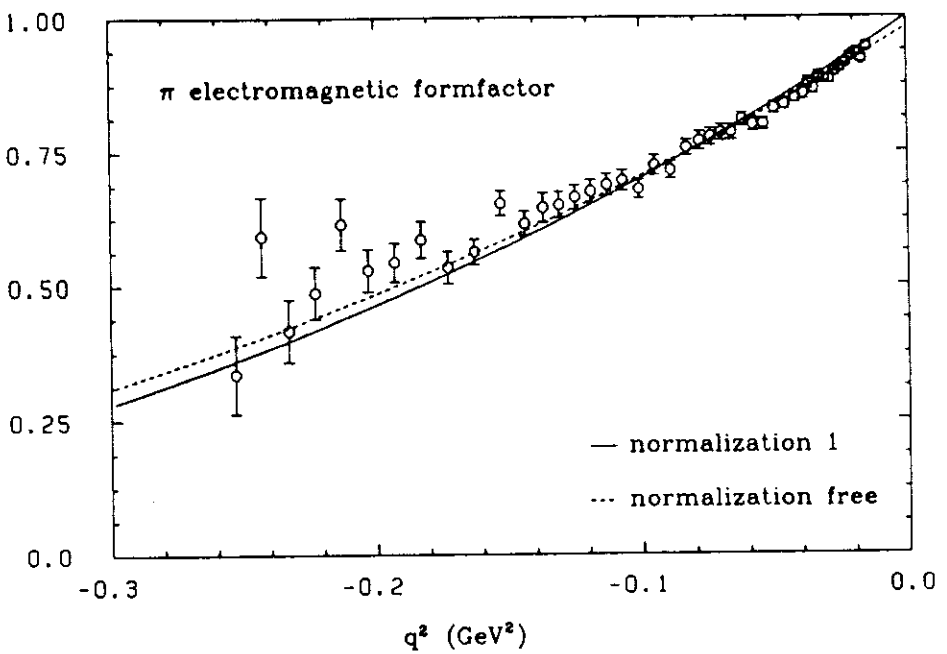
π electromagnetic formfactor
1.00
0.75
0.50
0.25
0.0
-0.3
-0.2
-0.1
0.0
q² (GeV²)
— normalization 1
··· normalization free

Fig. 2

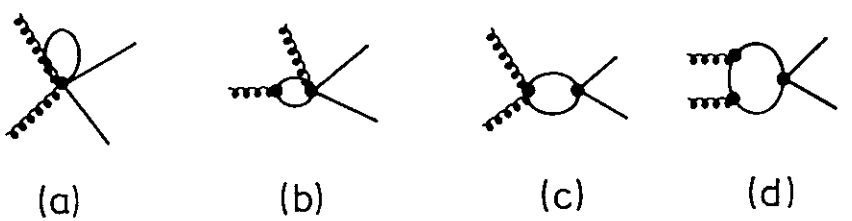
(a)
(b)
(c)
(d)

Fig. 3

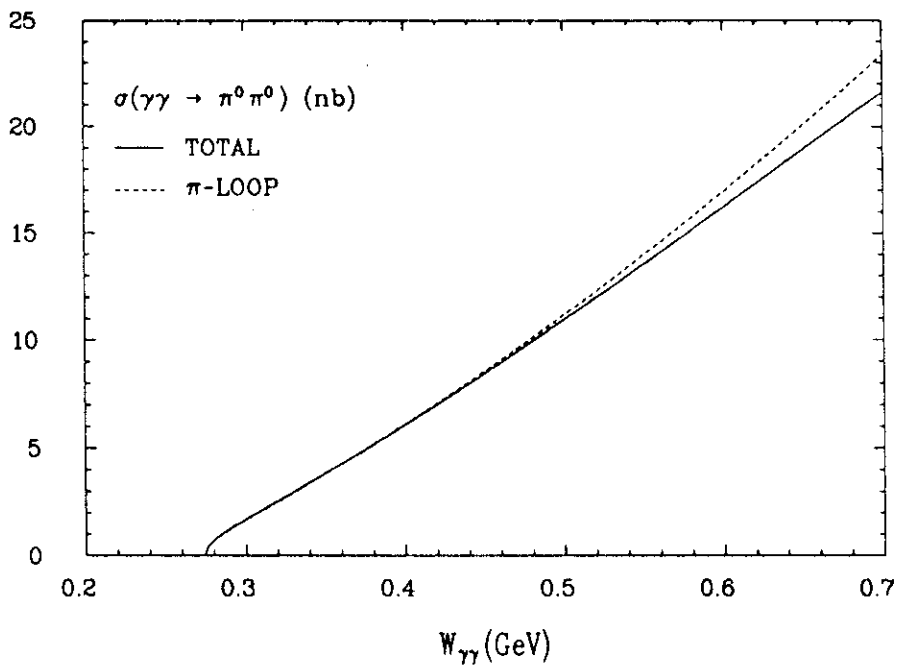
25
20
15
10
5
0
0.2
0.3
0.4
0.5
0.6
0.7
$\sigma(\gamma\gamma \to \pi^0\pi^0)$ (nb)
TOTAL
π-LOOP
$W_{\gamma\gamma}$(GeV)

Fig.4

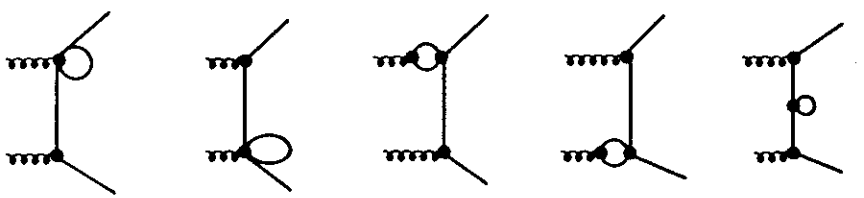

Fig.5

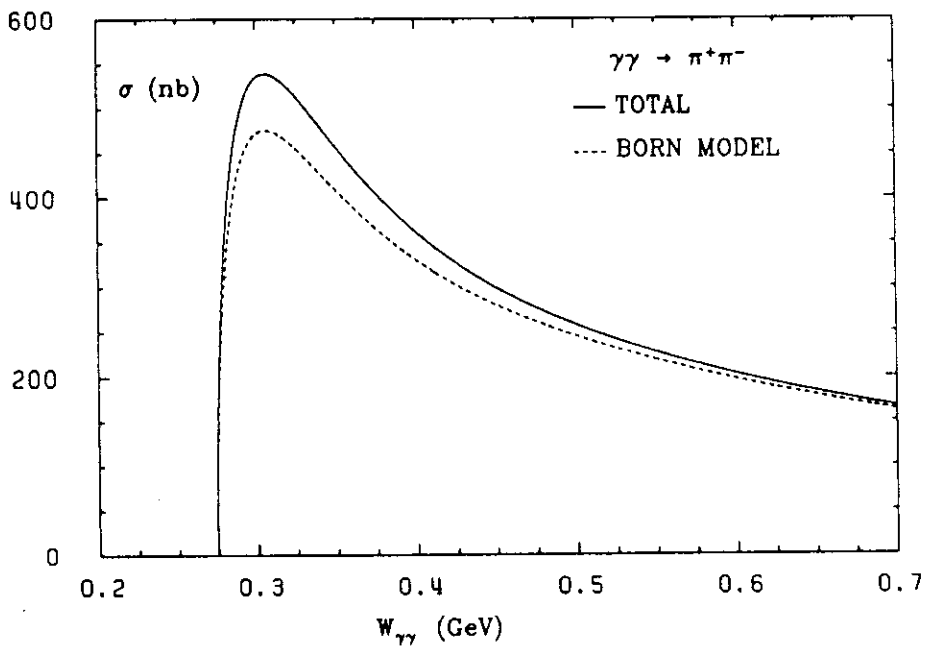
600
400
200
0
σ (nb)
γγ → π⁺π⁻
— TOTAL
---- BORN MODEL
0.2
0.3
0.4
0.5
0.6
0.7
W_γγ (GeV)

Fig.6

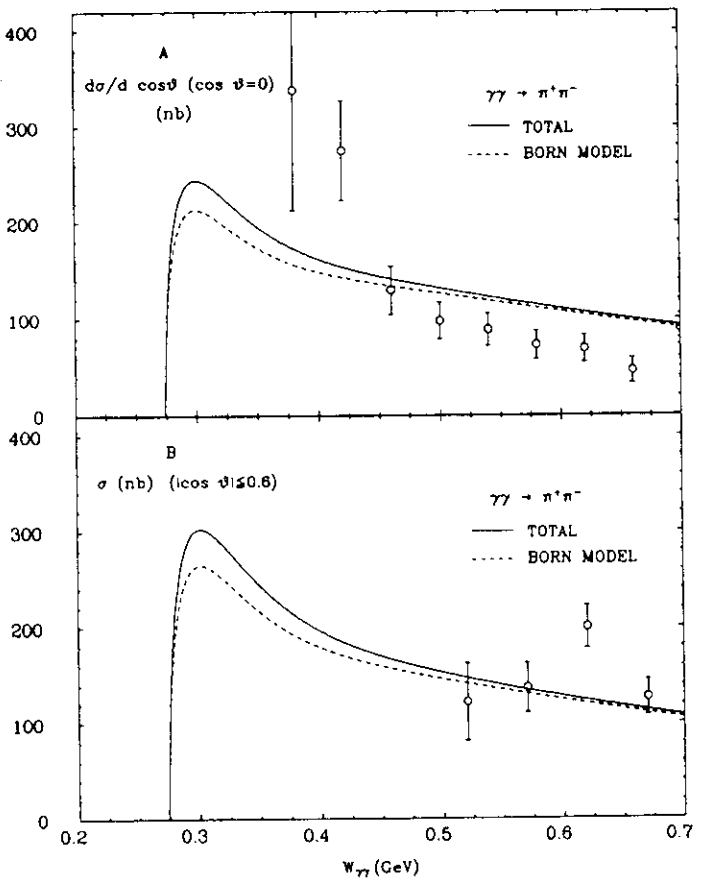
400
300
200
100
0
A
dσ/d cosϑ (cos ϑ=0)
(nb)
γγ → π⁺π⁻
TOTAL
BORN MODEL
400
300
200
100
0
B
σ (nb) (|cos ϑ|≤0.6)
γγ → π⁺π⁻
TOTAL
BORN MODEL
0.2
0.3
0.4
0.5
0.6
0.7
W_γγ (GeV)

Fig.7